Surface ecophysiological behavior across vegetation and moisture gradients in tropical South America

I.T. Baker[a,*], A.B. Harper[a], H.R. da Rocha[b], A.S. Denning[a], A.C. Araújo[c], L.S. Borma[d], H.C. Freitas[e], M.L. Goulden[f], A.O. Manzi[c], S.D. Miller[g], A.D. Nobre[c], N. Restrepo-Coupe[h], S.R. Saleska[h], R. Stöckli[i], C. von Randow[j], S.C. Wofsy[k]

[a]*Atmospheric Science Department, Colorado State University, Fort Collins, Colorado, USA.*
[b]*Departamento de cienciêas Atmosfericas, IAG, Universidade de São Paulo, São Paulo, Brazil.*
[c]*Embrapa Amazonia Oriental, Belém, Pará/Programa LBA, Instituto Nacional de Pesquisas da Amazônia, Manaus, Amazonas, Brazil*
[d]*Centro de Ciência do Sistema Terrestre/Instituto Nacional de Pesquisas Espaciais, São José dos Campos, São Paulo, Brazil*
[e]*Universidade de São Paulo, São Paulo, Brazil*
[f]*Department of Earth System Science, University of California, Irvine, California, USA.*
[g]*Atmospheric Sciences Research Center, State University of New York at Albany, Albany, New York, USA.*
[h]*Department of Ecology and Evolutionary Biology, University of Arizona, Tucson, Arizona, USA*
[i]*Climate Services, Climate Analysis, MeteoSwiss, Zurich, Switzerland*
[j]*Instituto Nacional de Pesquisas Espaciais, Cachoeira Paulista, São Paulo, Brazil*
[k]*Division of Applied Sciences, Harvard University, Cambridge MA, USA*

Abstract

Surface ecophysiology at five sites in tropical South America across vegetation and moisture gradients is investigated. From the moist northwest (Manaus) to the relatively dry southeast (Pé de Gigante, state of São Paulo) simulated seasonal cycles of latent and sensible heat, and carbon flux produced with the Simple Biosphere Model (SiB3) are confronted with observational data. In

*Corresponding Author: I.T. Baker, baker@atmos.colostate.edu

the northwest, abundant moisture is available, suggesting that the ecosystem is light-limited. In these wettest regions, Bowen ratio is consistently low, with little or no annual cycle. Carbon flux shows little or no annual cycle as well; efflux and uptake are determined by high-frequency variability in light and moisture availability. Moving downgradient in annual precipitation amount, dry season length is more clearly defined. In these regions, a dry season sink of carbon is observed and simulated. This sink is the result of the combination of increased photosynthetic production due to higher light levels, and decreased respiratory efflux due to soil drying. The differential response time of photosynthetic and respiratory processes produce observed annual cycles of net carbon flux. In drier regions, moisture and carbon fluxes are in-phase; there is carbon uptake during seasonal rains and efflux during the dry season. At the driest site, there is also a large annual cycle in latent and sensible heat flux.

1. Introduction

The Amazon Basin occupies a central position in our ability to understand and predict interactions between earth and atmosphere across multiple spatial and temporal scales. Surface-atmosphere exchange in this region is important to weather and climate both locally (Fu et al., 1999; Fu and Li, 2004; Li and Fu, 2004) and globally (Werth and Avissar, 2002; Schneider et al., 2006; Nobre et al., 2009). The dense forest and large spatial extent means this region stores a significant fraction of global terrestrial biomass

2

(Houghton et al., 2001), and a significant fraction of global species diversity as well (Malhi et al., 2008). It has been predicted that climate change may result in the conversion of large areas of the Amazonian forest to seasonal forest, savanna or grassland, releasing much of the carbon stored at the surface and further altering the radiation characteristics of the atmosphere (Cox et al., 2000; Huntingford et al., 2004; Huntingford et al., 2008). However, consensus has not been reached on total conversion fraction or spatial organization (Malhi et al., 2009; Salazar et al., 2007). Predictions such as these place a premium on our ability to understand the surface ecophysiology of tropical systems. If we are to predict global climate under changing radiative conditions, we must be able to translate our understanding of the physical system into numerical models, and tropical South America will play a significant role.

Recent work has debated which mechanism(s) are most responsible for determining variability in ecosystem function, and, due to the tight coupling between the vegetated surface and surface-atmosphere exchange, variability in exchange of energy, moisture and carbon between the atmosphere and terrestrial biosphere in the Amazon Basin. It has been proposed that Amazonian forests are light-limited, and respond to relative drought with an increase in ecophysiological function (Huete et al., 2006; Saleska et al., 2007). However, this finding has been challenged (Samanta et al., 2010), citing problems with cloud and aerosol masking of remotely-sensed vegetation characteristics (i.e. Sellers et al., 1996a, Los et al., 2000). Xu et al. (2011) discuss differential response in the areal extent and severity of Amazon Basin droughts in 2005 and 2010. Brando et al. (2010) discuss the possibility of differential response

3

across vegetation gradients as well as interactions between multiple processes (leaf production, carbon allocation, respiration, mortality) than can combine to produce apparently conflicting observations. As of this writing, we don't feel that the issue is closed.

Surface ecophysiology in Amazonia is tightly coupled to the atmosphere. Seasonal temperature range is small, and annual variability is primarily defined by the intensity and duration of wet and dry seasons. Bidirectional coupling between surface and atmosphere plays a critical role in timing, duration, and magnitude of seasonal rains, and the large areal extent of the basin provides Amazonia with influence on regional to global-scale circulation patterns (Gedney et al., 2000; Werth and Avissar, 2002). The region is important to global carbon flux, due to the large carbon stores and fluxes.

The behavior of the land surface is tightly coupled to the cycles of wet and dry seasons that define seasonality in the region. In the tropical Americas, there is an annual cycle, whereby convective precipitation associated with the Intertropical Convergence Zone (ITCZ) is centered over the Amazon Basin during austral summer (December, January, and February). In austral fall (March, April, May) this feature moves northward and westward to a position over Central America (Horel et al. 1989) where it remains during Boreal summer (June, July, August). The northward position of the precipitation maximum coincides with the wet season north of the equator; south of the equator, the wet season is approximately coincident with austral summer. At the latitudinal extremities of this precipitation oscillation (Central America and southeastern Brazil, approximately), annual precipitation variability is dominated by the annual cycle (Adler et al., 2003; Horel et al.,

1989). Between these spatial endpoints annual precipitation is larger, the dry season shorter or almost nonexistent, and interannual variability dominates the precipitation variance (Horel et al., 1989). Superimposed on this mean pattern is variability in circulation and vegetation behavior, which can be influenced by topography (Lu et al., 2005) or other factors such as soil depth or type (von Randow et al., 2004). Recycling, or the precipitation of water at a site or region that was locally evapotranspired rather than advected into the region, is an important component of the Amazonian hydrologic cycle and is estimated at 25-35% (Eltahir and Bras, 1994; Trenberth, 1999; Costa and Foley, 1999).

Seasonal cycles of observed water and heat flux across vegetation and moisture gradients from forest to savanna have been partitioned into two functional types (da Rocha et al., 2009; Costa et al., 2010). In regions where annual precipitation was large and dry season short, evaporation increased during seasonal drought. Latent heat flux was in phase with precipitation and evaporation decreased during the dry season in regions with a well-defined dry season and less annual precipitation. The authors in both papers postulated that wetter forests were light-limited, while evapotranspiration in drier regions was controlled by soil moisture.

In this manuscript, we simulate surface ecophysiology at a subset of the stations investigated by da Rocha et al. (2009). We evaluate the model's ability to reproduce observed annual mean behavior across vegetation and moisture gradients. Additionally, we integrate carbon flux into the analysis to investigate full ecosystem behavior. The goals of this study are to 1) demonstrate an ability to capture mean annual cycles of biophysical behav-

ior across vegetation and moisture gradients in model simulations, and 2) use the model's ability to partition processes into component behavior as a means to formulating more detailed conceptual descriptions of the mechanisms involved.

The paper is organized as follows: Methods, including model, sites, and data are introduced in Section 2. The behavior at individual sites is discussed in Section 3, summarized in Section 4, with conclusions in Section 5.

2. Methods

Historically, land surface models have had difficulty reproducing annual cycles of energy, moisture, and carbon flux in tropical ecosystems. Saleska et al. (2003) showed that several models inverted the annual carbon flux cycle when compared to observed data. Baker et al. (2008) demonstrated an ability to capture the mean annual cycle of energy, moisture and carbon fluxes, at a single point in the Tapajos River National Forest (Brazil), by incorporating observed mechanisms into the Simple Biosphere Model (SiB3). With that as a starting point, in this paper we again confront model results with observed quantities, this time at multiple sites and across vegetation and moisture gradients. We will focus on annual cycles of energy, moisture and carbon flux, but will evaluate behavior at shorter timescales to support conclusions where appropriate.

2.1. Model

The Simple Biosphere Model (SiB) was developed as a lower boundary for atmospheric models (Sellers et al., 1986), and has been coupled to General Circulation Models (GCMs; Sato et al., 1989; Randall et al., 1996) as

6

well as mesoscale models (Denning et al., 2003; Nicholls et al., 2004; Wang et al., 2007; Corbin et al., 2008). The addition of ecosystem metabolism to the code (Sellers et al., 1996a; Denning et al., 1996) gives the model a high degree of ecophysiological realism that is valuable to ecologists as well. SiB model output has been compared to eddy covariance observations at sites in midlatitude forest (Baker et al., 2003; Schaefer et al., 2008), grassland (Colello et al., 1998; Hanan et al., 2005), and tropical forest (Baker et al., 2008; Schaefer et al., 2008). The model has a proven track record for simulating exchange between the atmosphere and terrestrial biosphere, as evaluated in model intercomparison studies (Schwalm et al., 2010).

As a 'third generation' land surface scheme (Sellers et al., 1997), SiB incorporates ecophysiological function as an additional constraint on fluxes of latent (LE) and sensible (H) heat. Photosynthetic carbon assimilation is based on enzyme kinetics developed by Farquhar et al. (1980), and stomatal conductance couples vegetation behavior to the overall surface energy budget (Collatz et al., 1991; Collatz et al., 1992; Sellers et al., 1996a; Randall et al., 1996). Soil heat and moisture flux has been modified to follow the Community Land Model (CLM) (Dai et al., 2003). Root distribution follows Jackson et al. (1996), and a fully prognostic canopy air space (CAS) for temperature and moisture follows Baker et al. (2003) and Vidale and Stöckli (2005).

Long term Net Ecosystem Exchange (NEE) of carbon is the small residual between large photosynthetic and respiratory fluxes. In SiB, interannual NEE is constrained to zero (Denning et al., 1996) by constraining annual ecosystem respiration (autotrophic and heterotrophic) to the previous year's Gross Primary Productivity (GPP). This parameterization removes model

7

₁₃₃ dependence on carbon storage pools whose size may be unknown.

₁₃₄ Remotely-sensed information, such as Normalized Difference Vegetation
₁₃₅ Index (NDVI; Brown et al., 2004; Tucker et al., 2005; Pinzon et al., 2006)
₁₃₆ was introduced into SiB (Sellers et al., 1996a; Sellers et al., 1996b; Randall et
₁₃₇ al., 1996) to describe spatiotemporally variable vegetation phenology. NDVI
₁₃₈ is used to obtain values of Leaf Area Index (LAI) and fraction of Photosyn-
₁₃₉ thetically Active Radiation absorbed (fPAR) (Sellers et al., 1992, 1996b).
₁₄₀ Due to model formulation, fPAR is the more important quantity for deter-
₁₄₁ mination of potential photosynthesis and transpiration rates in SiB. At LAI
₁₄₂ values above 4 (m^2 leaf per m^2 ground), fPAR is nearly saturated (cf. Fig-
₁₄₃ ure 1 in Sellers et al., 1992), meaning that meteorological and soil moisture
₁₄₄ variability will play a larger role to determine ecophysiological response in
₁₄₅ densely vegetated regions such as tropical forests. As observed LAI in South
₁₄₆ American tropical forest is usually above $\approx$4 (Myneni et al., 2007; Malhado
₁₄₇ et al., 2009; Miller et al., 2004), SiB is not acutely responsive to variability in
₁₄₈ LAI in these regions. In other vegetation types where LAI/fPAR are lower
₁₄₉ (such as southeast Brazil), simulated quantities show a stronger correlation
₁₅₀ with spectral vegetation indices.

₁₅₁ Modifications to the code since SiB2 was introduced in 1996 (Sellers et
₁₅₂ al., 1996a; Sellers et al., 1996b) have been described elsewhere (Baker et
₁₅₃ al., 2003, 2008; Hanan et al., 2005; Vidale and Stöckli, 2005). Baker et
₁₅₄ al. (2008) identified several mechanisms that were required for the model to
₁₅₅ capture the annual cycles of energy, moisture, and carbon flux at the K83
₁₅₆ site in the Tapajos River National Forest. They are:

₁₅₇ • A soil reservoir large enough to store sufficient moisture to sustain eco-

8

physiological function through periodic drought. Most land surface models have a soil depth of 3-4 meters, which was found to be inadequate. A 10-meter deep soil was found to be sufficient at the Tapajos River K83 site, and has been incorporated into SiB as the standard.

- Adequate soil moisture is a necessary, but not sufficient mechanism to allow vegetation function to survive seasonal drought. Removal of water by roots, usually tied directly to root mass with depth in models, must be relaxed to allow water extraction by deep roots in excess of the amount suggested by root fraction. This phenomenon has been observed in multiple species (Oliveira et al., 2005), and allows retrieval of water stored deep in the soil. In SiB, we have developed a 'relative root fraction' system, wherein soil is extracted based on root density when water is plentiful. When surface soil (where the majority of root mass resides) dries, deeper roots are allowed to extract water at a rate exceeding their absolute root density.

Global maps of soil depth are nonexistent or unreliable, so SiB employs rooting depth as a mechanism to impose heterogeneity on a global 10-meter deep soil. Maximum rooting depth of different vegetation is described in Canadell et al. (1996), while Jackson et al., (1996) give a global map of rooting depth and distribution associated with discrete biome classes.

It has been postulated that hydraulic redistribution, or the movement of water across moisture gradients via roots, plays an important role in Amazonian forests' ability to survive seasonal drought (Lee et al., 2005). In this case hydraulic redistribution facilitates the movement of water downward during wet periods, increasing soil storage, and moves water upwards,

9

against gravity, rewetting surface soils during seasonal drought. We do not consider hydraulic redistribution in our simulations for two reasons: 1) previous simulations (Baker et al., 2008) show that hydraulic redistribution alone is not sufficient to reproduce observed seasonality in SiB, and 2) simulating hydraulic redistribution requires soil-to-root exchange coefficients that are unknown without detailed soil/root surveys. We call the current version of the model SiB3.

2.2. Observation Sites

The behavior of observed energy and moisture fluxes across vegetation and precipitation gradients in Amazonia was described in da Rocha et al., 2009), using data from seven stations in Brazil. We simulated ecophysiological behavior at 5 of these 7 sites, listed in order of decreasing mean annual precipitation: Manaus (K34), Jaru (RJA), Tapajos River National Forest (K67 and K83), and Pé de Gigante (PEG) (Fig. 1). All towers are in the Amazon basin except PEG, which is in São Paulo state. In the model, all sites are classified as evergreen forest except PEG, which is classified as seasonal forest. All sites were simulated for either 3 or 4 years over the period 2000-2005. Data availability for each site is shown in Fig. 2.

2.2.1. Data Availability

Numerical simulations require gap-filled meteorology (pressure, temperature, dewpoint, windspeed, longwave and shortwave radiation, and precipitation) as model inputs. Missing data were interpolated from neighboring values where gaps were short, and from climatology when gaps were long. Longwave radiation has a significant impact on surface behavior, and is spo-

radically measured at the sites used. Traditional techniques used to estimate longwave radiation at midlatitude sites are ineffective in the tropics; a new technique has been developed for determining incoming longwave (Restrepo-Coupe et al., 2012), and we use it here.

Model simulations were evaluated against measured flux of energy (sensible heat), moisture (latent heat), and carbon taken at the tower sites. However, not all observations are available at each site for all times; instrument failure, heavy rain, and low turbulence can all impair the ability of an eddy covariance instrument to accurately record data. NEE is the observation of choice for quantifying carbon sources and sinks of natural systems. This metric requires measurement of storage within the canopy air in addition to recording the flux of CO_2 past a sensor situated above treetop. The full measurement suite is available for some sites (i.e. K83; Miller et al., 2004), but the lack of observations of canopy CO_2 concentration at some other sites means that reliable NEE is not available everywhere. Furthermore, at K34 complex terrain has been identified as problematic to the calculation of NEE (von Randow et al., 2004). Therefore, we use observed carbon flux measured above the canopy, rather than NEE, as the observational constraint, to maintain consistency between sites. The prognostic canopy air space (Baker et al., 2003; Vidale and Stöckli, 2005) makes it possible for SiB3 to simulate the raw flux of CO_2 past a sensor. Canopy storage is accounted for in SiB3, so model flux of carbon is analogous to what the sensor sees. Since modeled NEE is constrained to a value of zero on an annual basis (Denning et al., 1996), we focus on the ability of eddy covariance instruments to detect change and/or ecosystem response to variability on multiple timescales, and

11

the ability of the model to reproduce this variability. We emphasize mean annual cycles in this study.

Evaluation of model simulations against eddy covariance flux observations can be problematic. Models are generally held to energy, moisture and trace gas conservation through the formulation of their governing equations. However, determination of energy balance closure in eddy covariance data has been an ongoing issue (Wilson et al., 2002; Hollinger et al., 2005; Foken et al., 2006). Furthermore, the lack of closure in the eddy covariance energy budget can imply lack of closure in observed carbon budget as well (Aranibar et al., 2006). The goal of this paper is not detailed analysis of observational techniques and data. Instead, we wish to exploit the acknowledged strength of eddy covariance observations to capture ecosystem response to *variability* in forcing over multiple timescales (diurnal, synoptic, monthly) for comparison to simulations.

Monthly-mean observed carbon flux shows a net negative value (terrestrial uptake) for almost all months at the stations evaluated here. However, it is well-known that drainage (Araújo et al., 2002), energy/carbon budget closure (von Randow et al., 2008), or the lack of storage observations all contribute uncertainty to observed carbon flux. Therefore, we calculate the monthly *anomaly* for comparing observed annual cycles of carbon flux to simulations. Anomaly in this context means the difference between the monthly value and the average over all months of the observational record. This metric neglects determination of observed source/sink on timescales longer than monthly, which is consistent with the annual balance property of SiB3 (Denning et al., 1996). Deviation from the monthly average carbon flux value is

also used in plots of daily average. No adjustment is made to observed latent or sensible heat flux.

3. Analysis

If we are to use a model to parse out elements of ecophysiological behavior, we must first evaluate the model against available observations. In this section we will show that SiB3 demonstrates competence when confronted with observational data across all 5 sites. Once established against observations, model representation of component mechanisms and interpretation of ecophysiological function will have more credence.

The mean seasonality (precipitation, radiation, temperature) at these sites is described in da Rocha et al. (2009), but will be briefly summarized here (Fig. 1), as a review of the climatological regime gives context to the discussion of biophysical behavior. Sites K34, K67 and K83 are all very near the equator, while RJA is located at approximately 10° south latitude. Site PEG is the farthest south, at approximately 20°. The wettest locations are in the north and west (K34, RJA), with a general decrease in annual mean precipitation towards the east and south. The driest site is PEG, in the southeast corner of the domain. The dry season is somewhat correlated with annual precipitation; K34 has a dry season, but its length is short (4 months, maximum) and monthly precipitation is frequently near or above the climatological definition of 100 mm month^{-1} for a 'dry month' (Keller et al., 2004) even during the dry season. There is a well-defined dry season at RJA of 5 months, even though annual precipitation is large, and 3 of these months (June, July and August) are extremely dry. Mean precipitation dur-

13

ing May and September at RJA is close to 100 mm. The Santarém sites (K83, K67) are similar to each other with regard to annual mean precipitation and length of dry season (5-6 months). Precipitation at these sites is not infrequent during dry months, and can exceed 100 mm during an individual month. At PEG the dry season is longer, and precipitation is rare or nonexistent during most dry months.

3.1. Manaus: K34

This tower is located in the Cuieiras reserve of the Instituto Nacional de Pesquisas da Amazónia (INPA), located approximately 60 km northwest of the city of Manaus, state of Amazonas. The site is described in detail by Araújo et al. (2002), its location is shown in Fig. 1 and data was collected from 2002-2005 (Fig. 2). Annual precipitation at K34 averages 2329 mm for the 4 years studied. Annual temperature variability is small, and both incoming and net radiation (R_{net}) is highest during the dry season (Fig. 1 and Fig. 3, panel a). Observed LE and H is nearly constant on an annual basis (Fig. 3, panel a), as is monthly carbon flux (Fig. 4, panel a). However, some cycle is evident: Observed LE, H and R_{net} all show maximum values during the dry season (Fig. 3 panel a). Observed carbon flux shows very little annual cycle, with maximum relative efflux late in the wet season, with slight relative uptake from late dry season through early wet season (Fig. 4 panel a).

Comparing model to observations at K34, we see that simulated R_{net} follows the seasonal cycle observed, with a consistent positive bias (Fig. 3, panel a). The overall energy budget of the model will reflect this bias, and can be almost completely accounted for by excess simulated H during the

14

wet season and excess LE during June-November (Fig. 3, panel a). Both observed and simulated ground heat flux (G, not shown) are very small, with absolute value on the order of 1-2 W m^{-2} or less. The annual cycle of model LE (Fig. 3,panel a) matches observed on a monthly basis. Simulated values are slightly higher, but maximum values occur during the wet season in both observations and simulation. Model H exceeds observed during the wet season (Fig. 3, panel a), and maximum model H takes place during the wet season, as opposed to the dry season in the observations. As in the observations, simulated H is less than LE, and amplitude of the annual cycle is small.

Simulated carbon flux closely matches the mean annual cycle observed (Fig. 4, panel a). Amplitude is small, with relative uptake in January and in July-August. Simulated GPP and total respiration (Fig. 4, panel a) are large and do not show obvious seasonality. There is a suggestion of larger simulated GPP during the dry season, but total respiration follows a similar path. Carbon flux lacks an obvious annual cycle in both model and observations, suggesting that relative direction of carbon flux (uptake or efflux) at K34 is a function of high-frequency variability in meteorological forcing (radiation, precipitation), on synoptic- to monthly timescales. This is supported by Fig. 5, which shows K34 daily-average values of LE, H, carbon flux, GPP/total respiration, and precipitation for February 2002. LE, in both model and observations, shows maximum values in the relatively dry periods between days 8-15 and 26-28. Modeled H follows observed generally, with a positive bias of between 10 and 25 W m^{-2} on a daily basis. This sensible heat bias is seen in the monthly average, shown in Fig. 3, (panel a). Modeled

15

carbon flux matches observed quite well on a daily basis, keeping in mind we are showing observed anomaly to emphasize response to changes in forcing rather than the absolute value of uptake or efflux. In the simulations, daily respiration is almost invariant during the month; relative uptake/efflux is determined by high-frequency variability in GPP, as vegetation responds to rapid changes in insolation. Since February is a very damp month, we expect soils to be very moist; the large, almost invariant respiration supports this. We might expect that the increased GPP during days 8-12 and following day 20 is responding to higher levels of light. Day 8 has very little precipitation, yet light levels are still low (only 3-4 hours with insolation greater than 300 W m^{-2}; not shown), resulting in low GPP. This type of high-frequency behavior is seen throughout the year.

Both observed and simulated behavior are consistent with a light-limited environment. The temperature, humidity and soil moisture regimes are favorable for both photosynthesis and respiration year-round, as indicated by the large gross fluxes and lack of seasonal cycles shown in Fig. 4 (panel a). During the dry season, reduced precipitation is associated with higher radiation levels, which elevates GPP. This response can also occur during short dry periods in other months. Increased insolation is also correlated with slightly elevated temperatures, which can enhance surface respiratory processes. It appears that GPP responds more rapidly than respiration to changes in forcing, so that short-term variability and the lag in respiration response combine to create short-term, small amplitude net fluxes of carbon that lack an obvious seasonal cycle.

3.2. Tapajos River National Forest: K67, K83

The K67 and K83 sites are located in Tapajos River National Forest, approximately 70 km south of the city of Santarém, Pará, Brazil (Fig. 1). These sites are described by Saleska et al., (2003), da Rocha et al. (2004), Miller et al. (2004), Goulden et al. (2004), and Hutyra et al., (2007). The Tapajos sites, while quite close to each other (within 20 km or so), are distinct in that K83 was selectively logged beginning in 2001, during the period used in this study. K83 and K67 have been considered simultaneously in other studies: Saleska et al., (2003) considered data prior to logging, but Costa et al. (2010) do not distinguish between logged and non-logged intervals. This is supported by Miller et al. (2007, 2011) who report that the selective logging at K83 does not appreciably influence observed fluxes of carbon and energy when compared to K67. For this study we will consider K67 and K83 in combination.

Latent heat flux, both observed and simulated (Fig. 3, panels b and c), increases at the outset of the dry season and decreases slightly as seasonal drought progresses. Interestingly, simulated H exceeds observed at K67 significantly in the wet season, and only slightly in the dry season, although simulated R_{net} is similar to observed. At K83, simulated wet season H is close to observed, and overestimated during the dry season, but observed R_{net} exceeds simulated.

At these sites, an annual cycle in carbon flux has been observed (Saleska et al., 2003), wherein there is regular carbon efflux during the wet season and uptake during seasonal drought. Our simulations, corroborated by observed carbon flux (Fig. 4, panels b and c), shows annual amplitude of 80-100 g

17

C m^{-2} in both the GPP and respiration cycles, but with a shift in phase that determines the annual carbon flux signal. Maximum respiratory flux at the Tapajos River sites occurs late in the wet season or soon after rains have diminished; soils are at maximum moisture levels, and increased temperature warms the soil slightly (temperature cycle shown in Fig. 1 b and c). Without replenishing rains, surface litter and near-surface soil dries out, and respiration decreases. Annual minimum respiration occurs just prior to the onset of the rainy season. Photosynthetic processes show a similar annual cycle in amplitude, but phase-lagged to respiration by 2-3 months. Respiration is quickly responsive to cessation of rainfall, while mechanisms described in Section 2 allow forest ecophysiological function to be maintained for longer periods. This difference in response time, coupled with the annual rainfall amount, soil depth, and length of dry season determine the annual cycle in carbon flux.

3.3. Reserva Jaru: RJA

The forest site at RJA, located 100 km north of Ji-Paraná in Rondônia state, Brazil (location shown in Fig. 1), is described by von Randow et al. (2004) and Andreae et al. (2002). von Randow et al. (2004) report a relatively thin soil at RJA, with depth less than 4 meters overlying a solid bedrock layer. For this reason we did not incorporate the deep soil modifications at this site, as reported in Baker et al. (2008) and Section 2. We retained the root mechanisms for water extraction as discussed in Baker et al. (2008), but limited soil depth to approximately 3.5 meters.

Mean annual precipitation at RJA is large (2354 mm yr^{-1} for the years used in this study), but latitude (10° South), thin soil and pronounced dry

18

season lead to differences in ecophysiological function when compared to K34. At RJA, wet season insolation is greater than K34 (Fig. 1, panel d) due to slightly longer day length. Dry season day length at RJA is slightly shorter than at K34, and midday insolation less as well. The seasonal cycle of net radiation displays a bimodal nature (Fig. 3, panel d), with maxima at the end of the wet and dry seasons. Modeled R_{net} captures the annual cycle, with a regular bias of 20-50 W m^{-2} on a monthly basis.

Mean annual cycles of observed LE and H (Fig. 3, panel d) reveal limited seasonality. LE is almost constant annually, with a slight increase in magnitude in September and October, at the end of the dry or beginning of the wet season. Amplitude of the annual H cycle is small, with small increases corresponding to the relative maxima in R_{net} at the end of the dry and wet seasons. Simulated LE is relatively constant and slightly larger than observed. However, the modeled LE decreases slightly at the end of the dry season, where observed LE increases. Simulated H shows seasonal maxima consistent with observed, but amplitude of the annual cycle is overestimated in addition to a positive bias.

The observed annual cycle of carbon flux anomaly is similar to K34, showing little variability throughout the year (Fig. 4, panel d). There are relative tendencies towards efflux at the end of the dry and wet seasons, with relative minima (uptake) at the midpoint of the year. Simulated carbon flux reproduces this general pattern, but overestimates the amplitude. Model GPP has a significant annual amplitude, reflecting the inability of the shallow soil to store sufficient moisture to maintain ecophysiological function completely through annual drought. Interestingly, simulated LE does not respond as

19

strongly as photosynthesis. From wet to dry seasons, gradients in water vapor pressure from the canopy to boundary layer are maintained, even as overall humidity decreases. At RJA, at the very end of the dry season a slight decrease in LE is seen in the simulations. The large amplitude in simulated carbon flux (Fig. 4, panel d) is due to phase incoherence between photosynthetic and respiratory response. Following the method outlined in Baker et al. (2008), respiration is tightly linked to moisture levels in near-surface soil; litter respiration is responsive to surface soil moisture levels, and relative root mass is greater near the surface as well. As surface moisture is depleted at dry season onset, total respiration decreases. There is no concurrent decrease in GPP, as roots are able to access water at deeper levels in the soil. It is only after several dry months, when total column soil moisture has been depleted, that GPP decreases. The lack of a large annual cycle in the observed carbon flux suggests that either the GPP and respiration cycles are more tightly in phase, or else there is much less amplitude in actual annual cycles than the model implies.

The hysteresis between morning and afternoon ecophysiological function, as reflected by diurnal cycles of latent heat and carbon flux, has been attributed to a circadian response in vegetation (Keller et al., 2004). This feature is seen across multiple sites, but we limit model evaluation of this feature to RJA. The model does not parameterize a purely circadian response, but imposes stress on potential photosynthesis by temperature, humidity, and soil moisture factors as described in Sellers et al. (1992). Simulated soil moisture stress operates on timescales of moistening and drying around precipitation events, but temperature and humidity stress operate in regular

20

diurnal cycles. We can explore the diurnal nature of the vegetation response (and compare simulated to natural processes) by plotting monthly-mean diurnal cycles of carbon flux against monthly-mean diurnal cycles of latent heat (Fig. 6). Hours 9, 12 and 16 are plotted as a triangles on the observed cycle, and we can see that the observed LE/Carbon flux cycle in the wet season (panel A) moves in a 'counterclockwise' direction; LE increases following sunrise concurrently with carbon uptake. In the afternoon, the process is reversed (concurrent decrease in LE and carbon uptake), but shifted slightly towards larger latent heat. This is due to a buildup in water vapor pressure in the CAS during the day. There is not a concurrent increase in the carbon uptake during the day: Increased daytime respiration and mixing of high-CO_2 air into the CAS from the atmosphere combine, with the result that CAS CO_2 levels reach a minimum value shortly after daybreak and remain at or near that value during the day, with less change in the CO_2 gradient between canopy air and the boundary layer. The simulated cycle, shown as a dashed line (hours not shown), shows a similar 'counterclockwise' pattern as was observed. However, the simulated cycle precedes the observed by several hours. For example, at 0900 the observed carbon flux is nearly neutral, but the simulation shows an uptake of 15 μmol m^{-2} sec^{-1}. This lag decreases somewhat during the day, so that by 1600 the observed and simulated values are quite similar. During the dry season (Fig. 6, panel B), both observed and simulated carbon flux/LE patterns resemble a 'figure-8'. In the morning, carbon uptake is strong while latent flux increase is minimal, due to much lower water vapor pressure (in both the CAS and atmosphere) when compared to the wet season. In the afternoon, latent heat flux decreases more

21

rapidly than carbon uptake, resulting in a 'figure-8' diel pattern. Again, the simulated cycle, while displaying the same diurnal cycle, precedes the observed by several hours, and modeled maximum carbon uptake in September is underestimated.

3.4. Cerrado; Pé de Gigante (PEG)

Carbon, energy, and moisture flux over a woodland savanna (cerrado Sensu stricto) site has been described by da Rocha et al. (2002), and da Rocha et al. (2009). The site is located in southeast Brazil, in São Paulo state, and has the largest temperature and radiation seasonality of all sites in this study (Fig. 1, panel e). Fluxes were recorded in Vassununga state park, in a region that contains closed canopy forest, and open shrubland in addition to woodland savanna.

Heterogeneity is a defining characteristic of savanna, and as such poses challenges for simulations. In SiB3, the use of satellite data to specify phenology requires a single-layer canopy (Sellers et al. 1996a, 1996b), so explicit representation of heterogeneous assemblages of grasses, shrubs and trees is not possible. The site is simulated as seasonal forest in SiB3. However, the spectral characteristics of NDVI captures the inclusion of grass phenology to a degree.

The Pé de Gigante site is water-limited (da Rocha et al., 2002; da Rocha et al. 2009), meaning that ecophysiological function is tightly coupled to precipitation and soil moisture. In contrast to all the other sites, where incoming radiation is regulated by cloud amount, seasonality at PEG is also defined by latitude. The dry season occurs during austral winter, so that radiation levels are actually higher during the rainy season, and temperatures

22

are warmer (Fig. 1 panel e). Latent heat is larger than sensible heat during the seasonal rains, but the Bowen ratio drops below one for a short period at the end of the dry season in both simulations and observations (Fig. 3, panel e).

Simulations and observations (Fig. 4, panel e) suggest relative uptake of carbon at PEG until early in the dry season, at which time respiration exceeds GPP. Simulations show that GPP drops rapidly following cessation of seasonal rains, while respiration subsides at a lower rate. This is in contrast to the ecophysiological mechanisms postulated for forest sites, where the opposite occurs; GPP is maintained during the dry season while respiration decreases quickly following cessation of rains. Our model simulations suggest several reasons for this behavior at PEG, including 1) reduced annual precipitation and longer, more severe (meaning very few precipitation events) dry season result in smaller water storage in the soil, 2) seasonal forests have shallower rooting systems than tropical evergreen forests (Jackson et al., 1996), and therefore lack the ability to access water stored deep in the soil. For these reasons, simulated GPP and respiration at PEG are in phase, and coupled tightly to water availability in the near-surface soil.

4. Discussion

We can summarize model performance with a review of model comparison to observed net radiation, latent and sensible heat flux, and carbon flux observed at the 5 stations. We acknowledge that simulated behavior does not match observed perfectly at these 5 diverse sites, but believe that our simulation results provide insight into physiological function. Furthermore,

very little local tuning to SiB3 was performed. We modified soil depth at RJA in accordance with local knowledge, but otherwise values from global maps were used to determine model parameters. These include vegetation and soil type, as well as parameters dependent on these values. These secondary parameters influence model components such as photosynthetic function and soil process (hydraulic and thermal conductivity). We use continuous spatial data sets as a means to facilitate regional- to global-scale simulation as an ultimate goal, rather than fine-tuning the model for local application.

No consistent bias in net radiation was found (Fig. 3). At three sites (K34, RJA and PEG) simulated R_{net} exceeded observed, at K83 observed exceeded simulated, and at K67 the correspondence was close. However, at all sites the mean annual cycle of observed and simulated was similar-where there was bias, the magnitude was nearly constant. We believe these differences are caused by the use of uniform tabular values in SiB3 to represent heterogeneous forests with diverse species, values of leaf angle distribution and radiative properties. Within a particular vegetation type (broadleaf evergreen forest, for example), heterogeneity in simulation canopy parameters will be imposed only by differences in spectrally-derived LAI/fPAR between the sites. In addition, SiB3 ingests a single incoming shortwave measurement and partitions it into visible/near-infrared and direct/diffuse partitions. We do not expect modeled albedo to exactly match observed in all cases.

Comparisons of simulated and observed latent heat flux follow net radiation trends at K34, K83, and RJA (Fig. 3). At K67 observed LE is slightly larger than simulated, and at PEG modeled and simulated LE are very similar in magnitude and annual cycle. At K34, K67 and K83 the annual cycles

24

are similar as well. At RJA there is very little amplitude in the annual cycle of LE, but simulations show a slight decrease at the end of the dry season where observations show a slight increase.

There is a positive bias in simulated sensible heat flux at all stations (Fig. 3). This has been noted in SiB simulations before (Baker et al., 2003), and is believe to be related to the leaf-to-canopy scaling scheme outlined in Sellers (1985). This bias is most notable in simulations of forests, such as are simulated in this study. Simulated annual cycles generally follow observed, and Bowen ratio, or relative magnitude of sensible to latent heat is consistent between model and observations.

Annual mean carbon flux is shown in Fig. 4. At K34 modeled and observed carbon flux has low amplitude and no obvious seasonality. At the Tapajos National Forest sites (K67, K83) the model captures the general form of the annual cycle (wet season efflux, dry season uptake), but precedes the time of uptake by one to 3 months. At RJA the model reproduces the basic form of the observed annual cycle, but with a larger amplitude, and at PEG SiB3 reproduces the observed carbon flux with reasonable fidelity.

Given the historical performance of land surface models in South America (cf. Fig. 2 in Saleska et al., 2003), we find these results to be very encouraging. We have simulated, with a minimum of localized tuning, the general form of annual cycles of energy, moisture, and carbon flux at several sites across Brazil. We believe these results provide some insight into the mechanistic coupling of carbon cycle processes that combine to determine annual cycles of flux across vegetation and moisture gradients.

5. Conclusions

Climatological control of ecophysiology is spatially heterogeneous in Brazil. da Rocha et al. (2009) showed that evapotranspiration in the wettest areas (central Amazon) is tightly linked to radiation levels (light-limited), while water availability regulates ET in the drier regions to the south and east. Our simulations reproduce this behavior. Forest sites K34, RJA, K67 and K83 maintain a consistently small Bowen ratio (sensible smaller than latent heat); maximum annual values for both H and LE occur during the dry season, when net radiation is greatest, and annual amplitude of LE/H cycles is relatively small. The dry season increase in both LE and H suggests an ecosystem response to increased radiation levels, without ecosystem stress, since evaporation is maintained. At the savanna site (PEG; simulated as a seasonal forest in SiB3), evaporation is tightly coupled to precipitation. Latent heat flux decreases immediately with cessation of seasonal rains, and Bowen ratio exceeds one during the dry season. Simulated annual cycle of latent and sensible heat at PEG is very similar to observed.

Vegetation couples carbon dynamics to the Bowen ratio by stomatal regulation of transpiration. Overall carbon flux is defined by the interaction of photosynthetic and respiratory processes. We've demonstrated that SiB3 can simulate observed annual cycles of carbon flux, and we use model diagnostics to partition GPP and respiration as a means to evaluate photosynthesis and respiration across vegetation and moisture gradients. We do not address overall source/sink of CO_2 on an annual or interannual basis for these individual sites. Local to regional-scale Net Ecosystem Exchange of CO_2 over long timescales is dependent upon storage pools, which are themselves the

residual from large gross photosynthetic and respiratory fluxes. These pools cannot be determined from model simulations performed on 3 or 4 years of observational data.

We find that a conceptual model of ecophysiological behavior emerges: In the wettest regions of the forest (K34), ecosystems are light- rather than water-limited. Gross carbon fluxes are continuously large, and small magnitude uptake or efflux is determined by high-frequency variability in forcing. A dry week, for example, may result in increased GPP due to higher light levels, while slight drying of near-surface soils may result in a small decrease in respiration. Moving downgradient in precipitation (K67, K83), annual total rainfall is less, and the dry season obtains definition. At these locations seasonality in carbon flux may be imposed by the mechanistic concepts outlined in Baker et al. (2008): A combination of GPP elevation in response to enhanced light levels and respiration decrease as surface soil desiccates results in carbon uptake during the dry season. At these sites, seasonality in carbon flux is distinct while seasonality in energy and moisture flux are minimal. Photosynthetic function is not excessively compromised during the seasonal drought, and transpiration maintains the Bowen ratio at small values. However, there is some suppression of GPP as the dry season progresses, indicating a combination of light- and water-limitation may be at work here. Using the terminology of Costa et al. (2010), we believe that here ET is controlled by a combination of abiotic (meteorological) and biotic (soil moisture deficit restricting canopy conductance) factors. At drier sites (PEG), vegetation has stress imposed upon it by the combination of even less annual precipitation and a longer dry season. The imposition of water

27

limitation in the drier regions has the effect of forcing the carbon cycle into phase with the precipitation cycle. Water limitation also has the effect of imposing larger amplitude to the annual cycles of latent and sensible heat flux. As vegetation experiences water stress, evapotranspiration rates cannot be maintained, and the Bowen ratio increases. This conceptual model is expressed in the GPP/Respiration cycles shown in Fig. 4.

Tropical forests survive annual drought (dry season), as well as climatological variability around mean annual cycles of wet and dry. Evapotranspiration is critical to precipitation recycling not only locally, but across regional and continental scales (van der Ent et al., 2010). It has been shown that simulations of atmospheric processes are responsive to improved physical realism at the land-atmosphere interface (Harper et al., 2010). The results of climate simulations that predict large-scale conversion of Amazonian forest to grassland or savanna (Cox et al., 2000; Betts et al., 2004; Cowling et al., 2004; Cox et al., 2004; Huntingford et al., 2004; Huntingford et al., 2008) will be more robust if they can show consistency with ecophysiological behavior under current conditions. It has been shown that land has more leverage than ocean in influencing the global atmospheric CO_2 growth rate (Friedlingstein et al., 2006, Baker et al., 2006, Gurney et al., 2008), and that the tropics play a major role in the land response. Therefore, fundamental understanding of tropical land surface response on a mechanistic level will be integral to our ability to predict both present-day climate and ecophysiological response to changing atmospheric forcing.

Our simulations have demonstrated an ability to rectify unrealistic ecophysiological stress in forest ecosystems (Saleska et al., 2003; Baker et al.,

28

2008) while maintaining reasonable response across vegetation and moisture gradients. But removing unrealistic stress on vegetation is only half of the battle; forests are conditioned to survive annual drought and, it is expected, anomalous drought as well. But if sustained drought in Amazonia occurs during the 21st century due to a higher incidence of El Niño conditions (Cattanio et al., 2002; Li et al., 2006) or a combination of climatological and sociological pressure on the ecosystem (Nepstad et al., 2008), it is realistic to expect that forest collapse, or a 'tipping point' may be reached (Nobre and Borma, 2009; Nepstad et al., 2008). Previously, models were unable to withstand even seasonal drought, in the form of a dry season. Now that we've adjusted our model physics to achieve greater resiliency to seasonal drought, we need to ensure that we have not created models that are impervious to drought.

6. acknowledgments

References

[1] Adler, R.F., G.J. Huffman, A. Chang, R. Ferraro, P. Xie, J. Janowiak, B. Rudolf, U. Schneider, S. Curtis, D. Bolvin, A. Gruber, J. Susskind, P. Arkin, and E. Nelkin, 2003. The Version 2 Global Precipitation Climatology Project (GPCP) monthly precipitation analysis (1979-Present). J. Hydrometeor., 4,1147-1167.

[2] Andreae M.O., Artaxo P., Brandão C., Carswell F.E., Ciccioli P., da Costa A.L., Culf A.D., Esteves J.L., Gash J.H.C., Grace J., Kabat P., Lelieveld J., Malhi Y., Manzi A.O., Meixner F.X., Nobre A.D., Nobre C., Ruivo M.L.P., Silva Dias M.A.F., Stefani P., Valentini R., von Jouanne J., Waterloo M.J., 2002. Biogeochemical cycling of carbon, water, energy, trace gases, and aerosols in Amazonia: The LBA-EUSTACH experiments. J. Geophys. Res. 107(D20): 8066, doi: 10.1029/2001JD000524.

[3] Aranibar, J.N., J.A. Berry, W.J. Riley, D.E. Patakis, B.E. Law, J.R. Ehleringer, 2006. Combining meteorology, eddy fluxes, isotope measurements, and modeling to understand environmental controls of carbon isotope discrimination at the canopy scale. Glob. Change Biol., 12, 710-730.

[4] Araújo, A.C., A.D. Nobre, B. Kruijt, J.A. Elbers, R. Dallarosa, P. Stefani, C. von Randow, A.O.Manzi, A.D. Culf, J.H.C. Gash, R. Velentini, P. Kabat, 2002. Comparative measurements of carbon dioxide fluxes from two nearby towers in a central Amazonian rainforest: The Manaus LBA site. J. Geophys. Res., 107(D20), 8090, doi:10.1029/2001JD000676.

[5] Baker, D.F., R.M. Law, K.R. Gurney, P. Rayner, P. Peylin, A.S. Den-

30

ning, P Bousquet, L. Bruhwiler, Y.-H. Chen, P. Ciais, I.Y. Fung, M. Heimann, J. John, T. Maki, S. Maksyutov, K. Masarie. M. Prather, B. Pak, I. Taguchi and Z. Zhu, 2006. TransCom 3 inversion intercomparison: Impact of transport model errors on the interannual variability of regions CO2 fluxes, 1988-2003. Global Biogeochem Cy., 20, GB1002, doi: 10.1029/2004GB002439.

[6] Baker, I.T., A.S. Denning, N. Hanan, L. Prihodko, P.-L. Vidale, K. Davis and P. Bakwin, 2003. Simulated and observed fluxes of sensible and latent heat and CO_2 at the WLEF-TV Tower using SiB2.5. Glob. Change Biol., 9, 1262-1277.

[7] Baker, I.T., L. Prihodko, A.S. Denning, M. Goulden, S. Milller and H. da Rocha, 2008. Seasonal drought stress in the Amazon: Reconciling models and observations. J. Geophys. Res., 113, G00B01, doi:10.1029/2007JG000644.

[8] Betts, R.A., P.M. Cox, M. Collins, P.P. Harris, C. Huntingford, C.D. Jones, 2004. The role of ecosystem-atmosphere interactions in simulated Amazonian precipitation decrease and forest dieback under global climate warming. Theor. Appl. Climatol., 78(1-3), 157-175.

[9] Brando, P.M., S.J. Goetz, A. BAccini, D.C. Nepstad, P.S.A. Beck, M.C. Christman, 2010. Seasonal and interannual variability of climate and vegetation indices across the Amazon. P. Natl. Acad. Sci. USA, 107(33), 14685-14690, doi:10.1037/pnas.0908741107.

[10] Brown, M.E., J. Pinzon and C.J. Tucker, 2004. New vegetation index dataset available to monitor global change. Eos Transactions, 85:565, 2004.

[11] Canadell, J., R.B. Jackson, J.R. Ehleringer, H.A. Mooney, O.E. Sala, E.D. Schulze, 1996. Maximum rooting depth of vegetation types at the global scale. Oecologia, 108(4), 583-595.

[12] Cattanio, J.H., E.A. Davidson, D.C. Nepstad, L.V. Verchot, I.L. Ackerman, 2002. Unexpected results of a pilot throughfall exclusion experiment on soil emissions of CO_2, CH_4, N_2O and NO in eastern Amazonia. Biol. Fert. Soils, 36(2), 102-108.

[13] Collatz, G.J., J.T. Ball, C. Grivet, J.A. Berry, 1991. Physiological and environmental regulation of stomatal conductance, photosynthesis and transpiration: A model that includes a laminar boundary layer. Agr. Forest Meteorol., 54, 107-136.

[14] Collatz, G.J., M. Ribas-Carbo, J.A. Berry, 1992. Coupled photosynthesis-stomatal conductance model for leaves of C4 plants. Aust. J. Plant Physiol., 19(5), 519-538.

[15] Colello, G.D., C.Grivet, P.J. Sellers and J.A. Berry, 1998. Modelig of energy, water and CO_2 flux in a temperate grassland ecosystem with SiB3: May-October 1987. J. Atmos. Sci., 55, 1141-1169.

[16] Corbin, K.D., A.S. Denning, L. Lu, J.-W. Wang and I.T. Baker, 2008. Possible representation errors in inversions of satellite CO_2 retrievals. J. Geophys. Res., 113, D02301, doi:10.1029/2007JD008716.

[17] Costa, M.H. and J.A. Foley, 1999. Trends in the hydrologic cycle of the Amazon basin. J. Geophys. Res., 104(D12), 14189-14198.

[18] Costa, M.H., M.C. Biajoli, L. Sanches, A.C.M. Malhado, L.R. Hutyra, H.R. da Rocha, R.G. Aguiar, A.C. de Araújo, 2010. Atmospheric versus vegetation controls of Amazonian tropical rain forest evapotranspiration: Are the wet and seasonally dry rain forests any different? J. Geophys. Res., 115, G04021, dpi:10.1029/2009JG001179.

[19] Cowling, S.A., R.A. Betts, P.M. Cox, V.J. Ettwein, C.D. Jones, M.A. Maslin, S.A. spall, 2004. Contrasting simulated past and future responses of the Amazonian forest to atmospheric change. Philos. T. Roy. Soc. B, 359(1443): 539-547.

[20] Cox, P.M., R.A. Betts,, C.D. Jones,, S.A. Spall,,I.J. Totterdell, 2000. Acceleration of global warming due to carbon-cycle feedbacks in a coupled climate model. Nature, 408, 9 November, 184-187.

[21] Cox, P.M., R.A. Betts, M. Collins, P.P. Harris, C. Huntingford, C.D. Jones, 2004. Amazonian forest dieback under climate-carbon cycle projections for the 21st century. Theor. Appl. Climatol., 78(1-3), 137-156.

[22] Dai, Y., X. Zeng, R.E. Dickinson, I. Baker, G. Bonan, M. Bosilovich, S. Denning, P. Dirmeyer, P. Houser, G. Niu, K. Oleson, A. Schlosser and Z.-L. Yang, 2003. The common land model (CLM). B. Am. Meteorol. Soc., 84, 1013-1023.

[23] da Rocha, H.R., H.C. Freitas, R. Rosolem, R. Juarez, R.N. Tannus, M.A. Ligo, O.M.R. Cabral, M.A.F. Silva Dias, 2002. Measurements of CO_2

exchange over a woodland savanna (Cerrado Sensu strictu) in southeast Brazil. Biota Neotropica, 2(1).

[24] da Rocha H.R., M.L. Goulden, S.D. Miller, M.C. Menton, L.D.V.O. Pinto, H.C. de Frietas, A.M. E Silva Figueira, 2004. Seasonality of water and heat fluxes over a tropical forest in eastern Amazonia. Ecol. Appl., 14(4) Supplement, S22-S32.

[25] da Rocha, H.R., A.O. Manzi, O.M. Cabral, S.D. Miller, M.L. Goulden, S.R. Saleska, N.R. Coupe, S.C. Wofsy, L.S. Borma, P. Artaxo, G. Vourlitis, J.S. Noguiera, F.L. Cardoso, A.D. Nobre, B. Kruijt, H.C. Frietas, C. von Randow, R.G. Aguiar, J.F. Maia, 2009. Patterns of water and heat flux across a biome gradient from tropical forest to savanna in Brazil. J. Geophys. Res., 114, G00B12, doi:10.1029/2007JG000640.

[26] Denning, A.S., G.J. Collatz, C. Zhang, D.A. Randall, J.A. Berry, P.J. Sellers, G.D. Colello, D.A. Dazlich, 1996. Simulations of terrestrial Carbon metabolism and atmospheric CO_2 in a general circulation model. Part 1: Surface carbon fluxes. Tellus B , 48B, 521-542.

[27] Denning, A.S., M. Nicholls, L. Prihodko, I. Baker, P.L. Vidale, K. Davis, P. Bakwin, 2003. Simiulated variations in atmospheric CO_2 over a Wisconsin forest using a coupled ecosystem-atmosphere model. Glob. Change Biol., 9(9), 1241-1250.

[28] Eltahir. E. and Bras, R.L., 1994. Precipitation recycling in the Amazon Basin. Q. J. Roy. Meteor. Soc., 120(518A), 861-880.

34

[29] Farquhar, G.D., S. von Caemmerer, J.A. Berry, 1980. A biochemical model of photosynthetic CO_2 assimilation in leaves of C3 species. Planta, 149, 78-90.

[30] Foken, T., F. Wimmer, M. Mauder, C. Thomas, C. Liebethal, 2006. Some aspects of the energy balance closure problem. Atmos. Chem. Phys., 6, 4395-4402.

[31] Friedlingstein, P.F., P. Cox, R. Betts, L. Bopp, W. von Bloh, V. Brovkin, P. Cadule, S. Doney, M. Eby. I. Fung, G. Bala, J. John, C. Jones, F. Joos, T. Kato, M. Kawamiya, W. Knoff, K. Lindsay, H.D. Matthews, T. Raddatz, P. Rayner, C. Reick, E. Roeckner, K.-G. Schnitzler, R. Schnur, K. Strassmann, A.J. Weaver, C. Yoshikawa, N. Zeng, 2006. Climate-carbon cycle feedback analysis: Results from the C^4MIP model intercomparison, J. Clim., 19, 3337-3353.

[32] Fu, R., B. Zhu, R.E. Dickinson, 1999. How do atmosphere and land surface influence seasonal changes of convection in the tropical amazon? J. Clim., 12(5), 1306-1321.

[33] Fu, R. and Li. W., 2004. The influence of the land surface on the transition from dry to wet season in Amazonia. Theor. Appl. Climatol., 78, 97-110, doi:10.1007/s00704-004-0046-7.

[34] Gedney, N., P.J. Valdes, 2000. The effect of Amazonian deforestation on the northern hemisphere circulation and climate. Geophys. Res. Let., 27(19), 3053-3056.

[35] Goulden, M.L., S.D. Miller, H.R. da Rocha, M.C. Menton, H.C. de Freitas, A.M. E Silva Figueira, C.A.D. de Sousa, 2004. Diel and seasonal patterns of tropical forest CO_2 exchange. Ecol. Appl., 14(4) Supplement, S42-S54.

[36] Gurney, K.R., D. Baker, P. Rayner and A.S. Denning, 2008. Interannual variations in continental-scale net carbon exchange and sensitivity to observing networks estimated from atmospheric CO_2 inversions for the period 1980 to 2005. Global Biogeochem Cy., 22(3), doi:10.1029/2007GB003082.

[37] Hanan, N.P., J.A. Berry, S.B. Verma, E.A. Walter-Shea, A.E. Suyker, G.G. Burba, A.S. Denning, 2005. Testing a model of CO_2, water and energy exchange in Great Plains tallgrass prairie and wheat ecosystems. Agr. Forest Meteorol., 131, 162-179.

[38] Harper, A.B., A.S. Denning, I.T. Baker, M.D. Branson, L. Prihodko, D.A. Randall, 2010. Role of deep soil moisture in modulating climate in the Amazon. Geophys. Res. Let., 37, L05802, doi:10.1029/2009GL042302.

[39] Hollinger, D.Y., Richardson, A.D., 2005. Uncertainty in eddy covariance measurements and its application to physiological models. Tree Physiol., 25(7), 873-885.

[40] Horel, J.D., A.N. Hahmann, J.E. Geisler, 1989. An investigation of the annual cycle of convective activity over the tropical Americas. J. Clim., 2(11), 1388-1403.

[41] Houghton, R.A., K.T. Lawrence, J.L. Hackler, S. Brown, 2001. The spa-

tial distribution of forest biomass in the Brazilian Amazon: A comparison of estimates. Glob. Change Biol., 7, 731-746.

[42] Huete, A.R., K. Didan, Y.E. Shimabukuro, P. Ratana, S.R. Salexska, L.R. Hutyra, W. Yang, R.R. Nemani, R. Myneni, 2006. Amazon rainforests green-up with sunlight in dry season. Geophys. Res. Let., 33, L06405, doi:10.1029/2005GL025583.

[43] Huntingford, C., P.P. Harris, N. Gedney, P.M. Cox, R.A. Betts, J.A. Marengo, J.H.C. Gash, 2004. Using a GCM analogue model to investigate the potential for Amazonian forest dieback. Theor. Appl. Climatol., 78(1-3): 177-185.

[44] Huntingford, C., R.A. Fisher, L. Mercado, B.B.B. Booth, S. Sitch, P.P. Harris, P.M. Cox, C.D. Jones, R.A. Betts, Y. Malhi, G.R. Harris, M. Collins, P. Moorcroft, 2008. Towards quantifying uncertainty in predictions of Amazon dieback. Philos. T. Roy. Soc. B, 363(1498): 1857-1864.

[45] Hutyra, L.R., J.W. Munger, S.R. Saleska, E. Gottleib, B.C. Daube, A.L. Dunn, D.F. Amaral, P.B. de Camargo, S.C. Wofsy, 2007. Seasonal controls on the exchange of carbon and water in an Amazonian rain forest. J. Geophys. Res., 112(G4), G04099, doi:10.1029/2007JG000573.

[46] Jackson, R.B., J. Canadell, J.R. Ehleringer, H.A. Mooney, O.E. Sala, E.D. Schulze, 1996. A global Analysis of root distributions for terrestrial biomes. Oecologia, 108, 389-411.

[47] Keller, M., A. Alencar, G.P. Asner, B. Braswell, M. Bustamante, E. Davidson, T. Feldpausch, E. Fernandes, M. Goulden, P. Kabat, B. Kruijt,

F. Luizao, S. Miller, D. Markewitz, A.D. Nobre, C.A. Nobre, N.P. Filho, H da Rocha, P. Silva Dias, C von Randow, G.L. Vourlitis, 2004. Ecological research in the Large-Scale Biosphere-Atmosphere Experiment in Amazonia: Early results. Ecol. Appl., 14(4) Supplement, S3-S16.

[48] Lee, J-E., R.S. Olivieira, T.E. Dawson, I. Fung, 2005. Root functioning modifies seasonal climate. P. Natl. Acad. Sci. USA, 102(49), 17576-17581, 6 December 2005.

[49] Lenters, J.D. and K.H. Cook, 1997. On the origin of the Bolivian high and related circulation features of the South American climate. J. Atmos. Sci., 54(5), 656-667.

[50] Li, W. and Fu. R., 2004. Transition of the large-scale atmospheric and land surface conditions from the dry to the wet season over Amazonia as diagnosed by the ECMWF re-analysis. J. Clim., 17(7), 2637-2651.

[51] Li, W. and R. Fu, 2006. Influence of cold air intrusions on the wet season onset over Amazonia. J. Clim., 19(2), 257-275.

[52] Los, S.O., G.J. Collatz, P.J. Sellers, C.M. Malmstrom, N.H. Pollack, R.S. DeFries, L. Bounoua, M.T. Parris, C.J. Tucker, D.A. Dazlich, 2000. A global 9-year biophysical land surface dataset from NOAA AVHRR data. J. Hydrometeor., 1, 183-199.

[53] Lu, L.X., A.S. Denning, M.A. da Silva-Dias, P. da Silva-Dias, M. Longo, S.R. Freitas, S. Saatchi, 2005. Mesosscale circulations and atmospheric CO_2 variations in the Tapajos region, Para, Brazil. J. Geophys. Res., 110(D21), D21101, doi:10.1029/2004JD005757.

38

[54] Malhado, A.C.M., M.H. Costa, F.Z. Lima, K.C. Portilho, D.N. Figueiredo, 2009. Seasonal leaf dynamics in an Amazonian tropical forest. Forest Ecol. Manag., 258(7), 1161-1165.

[55] Malhi, Y., J.T. Roberts, R.A. Betts, T.J. Killeen, W. Li, C.A. Nobre, 2008. Climate change, deforestation, and the fate of the Amazon. Science, 319, 169-172, doi:10.1126/science.1146961.

[56] Malhi, Y., L.E.O.C. Aragão, D.B. Metcalf, R. Paiva, C.A. Quesada, S. Almeida, L. Anderson, P. Brando, J.Q. Chambers, A.C.L. da Costa, L.R. Hutyra, P. Oliveira, S. Pati no, E.H. Pyle, A.L. Robertson, L.M. Teixeira, 2009. Comprehensive assessment of carbon productivity, allocation and storage in three Amazonian forests. Glob. Change Biol., doi:10.1111/j.1365-2486.2009.01780.x.

[57] Miller, S.D., M.L. Goulden,M.C. Menton,H.R. da Rocha, H.C. de Freitas,A.M.E.S. Figueira,C.A.D. de Sousa, 2004. Biometric and micrometeorological measurements of tropical forest carbon balance. Ecol. Appl.,14(4) Supplement, S114-S126.

[58] Miller, S.D., M.L. Goulden, H.R. da Rocha, 2007. The effect of canopy gaps on sub canopy ventilation and scalar fluxes in a tropical forest. Agr. Forest Meteorol., 142, 25-34, doi:10.1016/j.agrformet.2006.10.008.

[59] Miller, S.D., M.L. Goulden, L.R. Hutyra, M. Keller, S.R. Saleska, S.C. Wofsy, A.M.S. Figueira, H.R. da Rocha, P.B. de Camargo, 2011. Reduced impact logging minimally alters tropical rainforest carbon

and energy exchange. P. Natl. Acad. Sci. USA, 108(48), 19431-19435, doi:10.1073/pnas.1105068108.

[60] Myneni, R.B., W. Yang, R.R. Nemani, A.R. Huete, R.E. Dickinson, Y. Knyazikhin, K. Didan, R. Fu, R.I.N. Juarez, S.S. Saatchi, H. Hashimoto, K. Ichii, N.V. Shabanov, B. Tan, P. Ratana, J.L. Privette, J.T. Morisette, E.F. Vermote, D.P. Roy, R.E. Wolfe, M.A. Friedl, S.W. Running, P. Votava, N. El-Saleous, S. Devadiga, Y. su, V.V. Salomonson, 2007. Large seasonal swings in leaf area of Amazon rainforests. P. Natl. Acad. Sci. USA, 104(12), 4820-4823.

[61] Nepstad, D.C., C.M. Stickler, B. Soares-Filho, F. Merry, 2008. Interactions among Amazon land use, forests and climate: prospects for a near-term forest tipping point. Philos. T. Roy. Soc. B, 363(1498), 1737-1746.

[62] Nicholls, M.E., A.S. Denning, Prihodko, L., P.L. Vidale, I. Baker, K. Davis, P. Bakwin, 2004. A multiple-scale simulatin of variations in atmospheric carbon dioxide using a coupled biosphere-atmosphere model. J. Geophys. Res., 109(D18), D18117, doi:10.1029/2003JD004482.

[63] Nobre, C.A., and L.D.S. Borma, 2009. 'Tipping points' for the Amazon forest. Current Opinion in Environmental Sustainability, 1:28-36, doi:10.1016/j.cosust.2009.07.003.

[64] Nobre, P., M. Malagutti, D.F. Urbano, R.A.F de Almeida, E. Giarolla, 2009. Amazon deforestation and climate change in a couple model simulation. J. Clim., 22, 5685-5697, doi:10.1175/2009JCLI2757.1.

[65] Oliviera, R.S., T.E. Dawson, S.S.O. Burgess, D.C. Nepstad, 2005. Hydraulic redistribution in three Amazonian trees. Oecologia, 145, 354-363.

[66] Phillips, O.L., L.E.O.C. Aragão, S.L. Lewis, J.B. Fisher, J. Lloyd, G. López-González, Y. Mallhi, A. Monteagudo, J. Peacock, C.A. Quesada, G. van der Heijden, S. Almeida, I. Amaral, L. Arroyo, G. Aymard, T.R. Baker, O. Bánki, L. Blanc, D. Bonal, P. Brando, J. Chave, A.C.A. de Oliveria, N.D. Cardozo, C.I. Czimczik, T. R. Feldpausch, M.A. Freitas, E. Gloor, N. Higuchi, E. Jiminéz, G. Lloyd, P. Meir, C. Mendoza, A. Morel, D.A. Neill, D. Nepstad, S. Patiño, M.C. Peñuela, A. Prieto, R. Ramírez, M Schwarz, J. Silva, M Sllveira, A.S. Thoma, H ter Steege, J. Stropp, R. Aásquez, P. Zelazowski, E.A. Dávila, S. Andelman, A. ANdrade, K.-J. Chao, T.Erwind, A.Di Fiore, E. Honorio C., H. Keeling, T.J. Killeen, W.F. Laurance, A. Peña Cruz, N.C.A. Pitman, P.N. Vargas, R. Ramírez-Angulo, A. Rudas, R. Salamão, N. Silva, J. Terborgh, A. Torres-Lezama, 2009. Drought sensitivity of the Amazon forest. Science, 323, 1344-1347.

[67] Pinzon, J., M.E. Brown and C.J. Tucker, 2006. Satellite time series correction of orbital drift artifacts using empirical mode decomposition. In: Applications of Empirical Mode Decomposition, Chapter 10, Part II, Editor: Nordon Huang.

[68] Randall, D.A., D.A. Dazlich, C. Zhang, A.S. Denning, P.J. Sellers, C.J. Tucker, L. Bounoua, J.A. Berry, G.J. Collatz, C.B. Field, S.O. Los, C.O. Justice, I. Fung, 1996. A revised land surface parameterization (SiB2) for GCMs. Part III: The greening of the Colorado State University General Circulation Model. J. Clim., 9(4), 738-763.

[69] Restrepo-Coupe, N., X. Zeng, I. Baker, R. Rosolem, K. Sakaguchi, B. Christofferson, L.G. de Goncalves, M. Muza, A.C. da Araujo, O.M.R. Cabral, P.B. de Camargo, D.R. Fitzjarrald, M.L. Goulden, B. Kruijt, J.M.F. Maia A.O. Manzi, S.D. Miller, A.D. Nobre, C. von Randow, H.R. da Rocha, R.K. Sakai, J. Tota, G.B. Zanchi, S.R. Saleska, 2011a. An empirical model for downward longwave radiation applied at 6 of the Brasil flux network sites. Agr. Forest Meteorol., in review.

[70] Salati, E., A. Dallollio, E. Matsui, J.R. Gat, 1979. Recycling of water in the Amazon-Basin-Isotopic Study. Water Resour. Res., 15(5), 1250-1258.

[71] Salazar, L.F., C.A. Nobre, M.D. Oyama, 2007. Climate change consequences on the biome distribution in tropical South America. Geophys. Res. Let., 34, L09708, doi:10.1029/2007GL029695.

[72] Saleska, S.R., S.D. Miller, D.M. Matross, M.L. Goulden, S.C. Wofsy, H.R. da Rocha, P.B de Camargo, P. Crill, B.C. Dauge, H.C. de Frietas, L.R. Hutyra, M. Keller, V. Kirchoff, M. Menton, J.W. Munger, E.H. Pyle, A.H. Rice, H. Silva, 2003. Carbon in Amazon forests: Unexpected seasonal fluxes and disturbance-Induced losses. Science, 302, 1554-1557, 28 November 2003.

[73] Saleska, S.R., K. Didan, A.R. Huete, H.R. da Rocha, 2007. Amazon forests green-up during 2005 drought. Science, 318(5850), 612, doi:10.1126/science.1146663)

[74] Samanta, A. S. Ganguly, H. Hashimoto, S. Devadiga, E. Vermote, Y. Knyazikhin, R. R. Nemani, R.B. Myneni, 2010. Amazon forest did

967 not green-up during the 2005 drought. Geophys. Res. Let., 37, L05401,
968 doi:10.1029/2009GL042154.

969 [75] Sato, N. P.J. Sellers, D.A. Randall, E.K. Schneider, J. Shukla, J.L. Kin-
970 ter, Y.T. Hou, E. Albertazzi, 1989. Effects of implementing the Siimple
971 Biophere Model in a General Circulation Model. J. Atmos. Sci., 46(18),
972 2757-2782.

973 [76] Schaefer, K., G.J. Collatz, P. Tans, A.S. Denning, I. Baker,
974 J. Berry, L. Prihodko, N. Suits and A. Philpott, 2008. The
975 combined Simple Biosphere/Carnegie-Ames-Stanford Approach (SiB-
976 CASA) terrestrial carbon cycle model. J. Geophys. Res.,113, G03034,
977 doi:10.1029/2007JG000603.

978 [77] Schneider, E. K., M. Fan, B. P. Kirtman, and P. A. Dirmeyer, 2006:
979 Potential effects of Amazon deforestation on tropical climate. IGES/COLA
980 Rep., 41 pp.

981 [78] Schwalm, C.R., C.A. Williams, K. Schaefer, R. Anderson, M.A. Arain,
982 I. Baker, A. Barr, T.A. Black, G. Chen, J.M. Chen, P. Ciais, K.J. Davis,
983 A. Desai, M. Dietze, D. Dragoni, M.L. Fischer, L.B. Flanagan, R. Grant,
984 L. Gu, D. Hollinger, R.C. Izaurralde, C. Kucharik, P. Lafleur, B.E. Law,
985 L. Li, Z. Li, S. Liu, E. Lokupitya, Y. Luo, S. Ma, H. Margolis, R. Mata-
986 mala, H. McCaughey, R.K. Monson, W.C. Oechel, C. Peng, B. Poulter,
987 D.T. Price, D.M. Ricciutto, W. Riley, A.K. Sahoo, M. Sprintsin, J. Sun,
988 H. Tian, C. Tonitto, H. Verbeek and S.B. Verma, 2010. A model-data in-
989 tercomparison of CO_2 exchange across North America: Results from the

990   North American Carbon Program site synthesis. J. Geophys. Res., 115,
991   G00H05, doi:10.1029JG001229.

992 [79] Sellers, P.J., 1985. Canopy reflectance, photosynthesis and respiration.
993   Int. J. Remote Sens., 6(8), 1335-1372.

994 [80] Sellers, P.J., Y. Mintz, Y.C. Sud, A. Dalcher, 1986. A Simple Biosphere
995   Model (SiB) for use within General Circulation Models. J. Atmos. Sci.,
996   43(6), 505-531.

997 [81] Sellers, P.J., J.A. Berry, G.J. Collatz, C.B. Field, F.G. Hall, 1992.
998   Canopy reflectance, photosynthesis, and transpiration. III. A reanalysis
999   using improved leaf models and a new canopy integration scheme. Remote
1000   Sens. Environ., 42, 1878-216.

1001 [82] Sellers, P.J. D.A. Randall, G.J. Collatz, J.A. Berry, C.B. Field, D.A. Da-
1002   zlich, C. Zhang, G.D. Colello, L. Bounoua, 1996a. A revised land surface
1003   parameterization (SiB2) for Atmospheric GCMs. Part I: Model formula-
1004   tion. J. Clim., 9(4), 676-705.

1005 [83] Sellers, P.J. S.O. Los, C.J. Tucker, C.O. Justice, D.A. Dazlich, G.J.
1006   Collatz, D.A. Randall, 1996b. A revised land surface parameterization
1007   (SiB2) for Atmospheric GCMs. Part II: The generation of global fields
1008   of terrestrial biophysical parameters from satellite data. J. Clim., 9(4),
1009   706-737.

1010 [84] Sellers, P.J., R.E. Dickinson, D.A. Randall, A.K. Betts, F.G. Hall, J.A.
1011   Berry, G.J. Collatz, A.S. Denning, H.A. Mooney, C.A. Nobre, N. Sato,
1012   C.B. Field and A. Henderson-Sellers, 1997. Modeling the exchanges of

1013   energy, water, and carbon between continents and the atmosphere. Science,
1014   275, 502-509.

[85] Trenberth, K.E., 1999. Atmospheric moisture recycling: Role of advec-
1016   tion and local evaporation. J. Clim., 12(5), 1368-1381.

[86] Tucker, C.J., J.E. Pinzon, M.E. Brown, D.A. Slayback, E.W. Pak, R.
1018   Mahoney, E.F. Vermote, N. El Saleous, 2005. An extended AVHRR 8-km
1019   NDVI dataset compatible with MODIS and SPOT vegetation NDVI Data.
1020   Int. J. Remote Sens., 26(20), 4485-4498.

[87] van der Ent, R.J., H.H.G. Savenjie, B. Schaefli, S.C. Steele-Dunn, 2010.
1022   Origin and fate of atmospheric moisture over continents. Water Resour.
1023   Res., 46, doi:10.1029/2010/WR009127.

[88] Vidale, P.L., Stöckli, R., 2003. Prognostic canopy air solutions for land
1025   surface exchanges.Theor. Appl. Climatol., 80, 245-257.

[89] von Randow, C., A.O. Manzi, B. Kruijt, P.J. de Oliveira, F.B. Zanchi,
1027   R.L. Silva, M.G. Hodnett, J.H.C. Gash, J.A. Elbers, M.J. Waterloo, F.L.
1028   Cardoso, P. Kabat, 2004. Comparative measurements and seasonal varia-
1029   tions in energy and carbon exchange over forest and pasture in South West
1030   Amazonia. Theor. Appl. Climatol., 78, 5-26.

[90] von Randow, C., B. Kruijt, A.A.M. Holtslag, M.B.L.Oliveira, 2008. Ex-
1032   ploring eddy-covariance and large-aperture scintillometer measurements in
1033   an Amazonian rain forest. Agr. Forest Meteorol., 148(4), 680-690.

[91] Wang, J.W., A.S. Denning, L. Lu, I.T. Baker, K.D. Corbin, K.J.

1035   Davis, 2007. Observations and simulations of synoptic, regional, and lo-

1036   cal variations in atmospheric CO_2. J. Geophys. Res., 112(D4), D0418,

1037   doi:10.1029/2006JD007410.

1038 [92] Werth, D., R. Avissar, 2002. The local and global effects of Amazon de-

1039   forestation. J. Geophys. Res., 107(D20), 087, doi:10.1029/2001JD000717.

1040 [93] Wilson, K., A. Goldstein, E. Falge, M. Aubinet, D. Baldocchi, P.

1041   Berbigier, C. Bernhofer, R. Ceulemans, H. Dolman, C. Field, A. Grelle,

1042   A. Ibrom, B.E. Law, A. Kowalski, T. Meyers, J. Moncrieff, R. Monson,

1043   W. Oechel,. J. Tenhunen, R. Valentini, S. Verma, 2002. Energy balance

1044   closure at FLUXNET sites. Agr. Forest Meteorol., 113, 223-243.

1045 [94] Xu, L., A. Samanta, M.H. Costa, S. Ganguly, R.R. Nemani, R.B.

1046   Myneni, 2011: Widespread decline in greenness of Amazonian veg-

1047   etation due to the 2010 drought. Geophys. Res. Let., 38, L07402,

1048   doi:10.1029/2011GL046824.

Figure 1: Site location and mean monthly incoming shortwave radiation, temperature and precipitation, following Figure 1 of da Rocha et al. (2009). Dry season, defined as number of months with less than 100 mm of precipitation, is shaded, and a dashed line indicates 10 cm (100 mm) of precipitation. Annual mean precipitation for the years used in this study is listed at the top of each panel.

Figure 2: Data availability for the sites used in this study.

Figure 3: Mean annual cycles of modeled and observed net radiation (Rnet), latent heat (LE), and sensible heat (H) for the 5 stations superimposed on a histogram of monthly-mean precipitation. Locations are shown in Figure 1, dry season is shaded as before.

Figure 4: Mean annual cycles of modeled and observed carbon flux for the 5 stations, superimposed on a histogram of monthly-mean precipitation. Locations of towers are shown in Figure 1. Modeled Gross Primary Productivity (GPP) and total respiration are shown at the top of each panel; dry season is shaded.

Figure 5: Daily mean (modeled and observed) Latent, Sensible and Carbon flux for the month of February 2002 at K34 (Panels A-C) Observations are shown as solid lines with symbols, simulated value as solid lines. Modeled partition of Carbon flux is shown in Panel D, daily precipitation in Panel E.

Figure 6: Monthly-mean diurnal composite of Latent Heat (X-axis) plotted against Carbon flux (Y-axis) for RJA, March (panel A) and September (panel B) 2000. Hours 9, 12, and 16 are indicated with triangles in the observations.
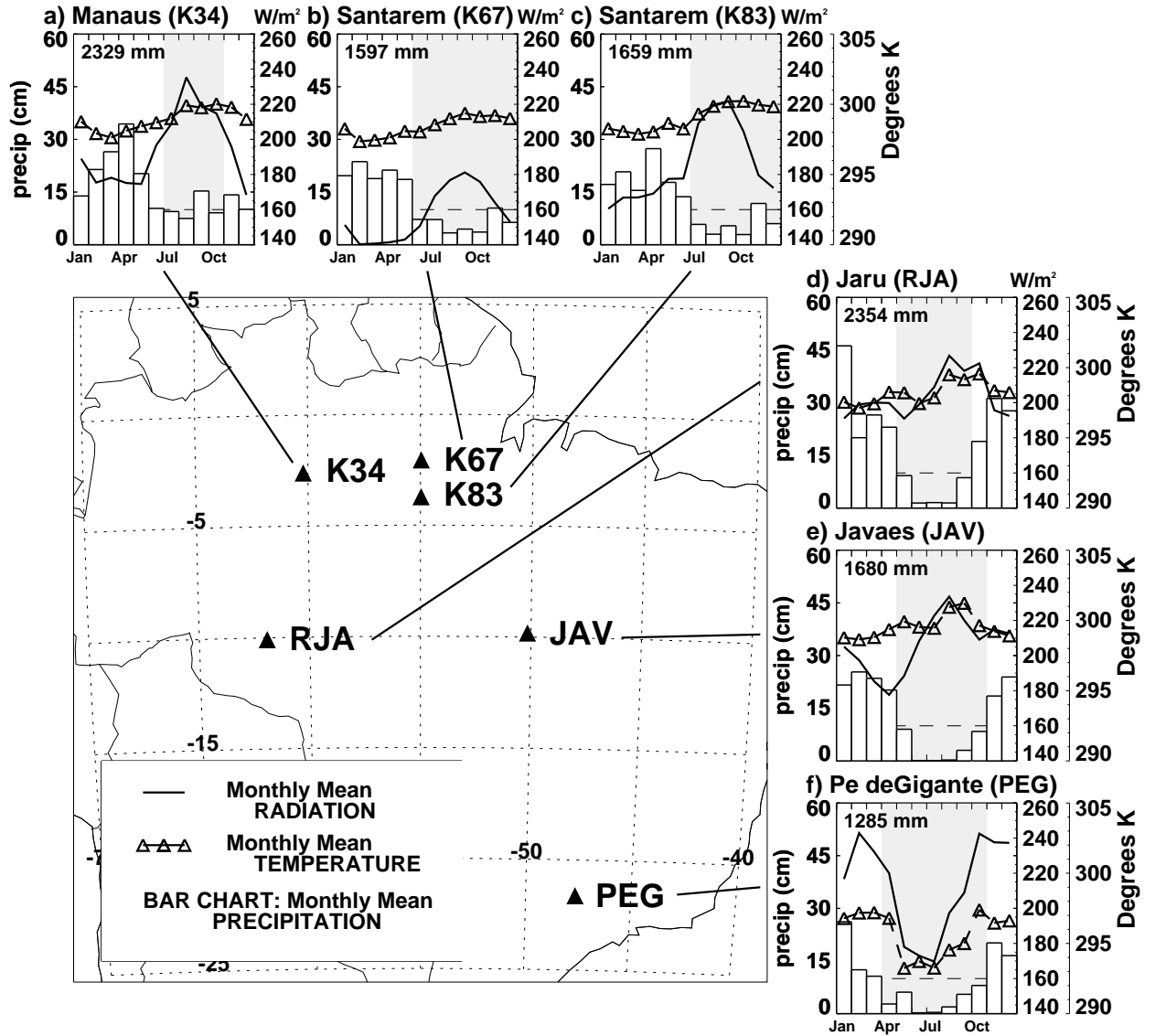
Figure 1: Site location and mean monthly incoming shortwave radiation, temperature and precipitation, following Figure 1 of da Rocha et al. (2009). Dry season, defined as number of months with less than 100 mm of precipitation, is shaded, and a dashed line indicates 10 cm (100 mm) of precipitation. Annual mean precipitation for the years used in this study is listed at the top of each panel.

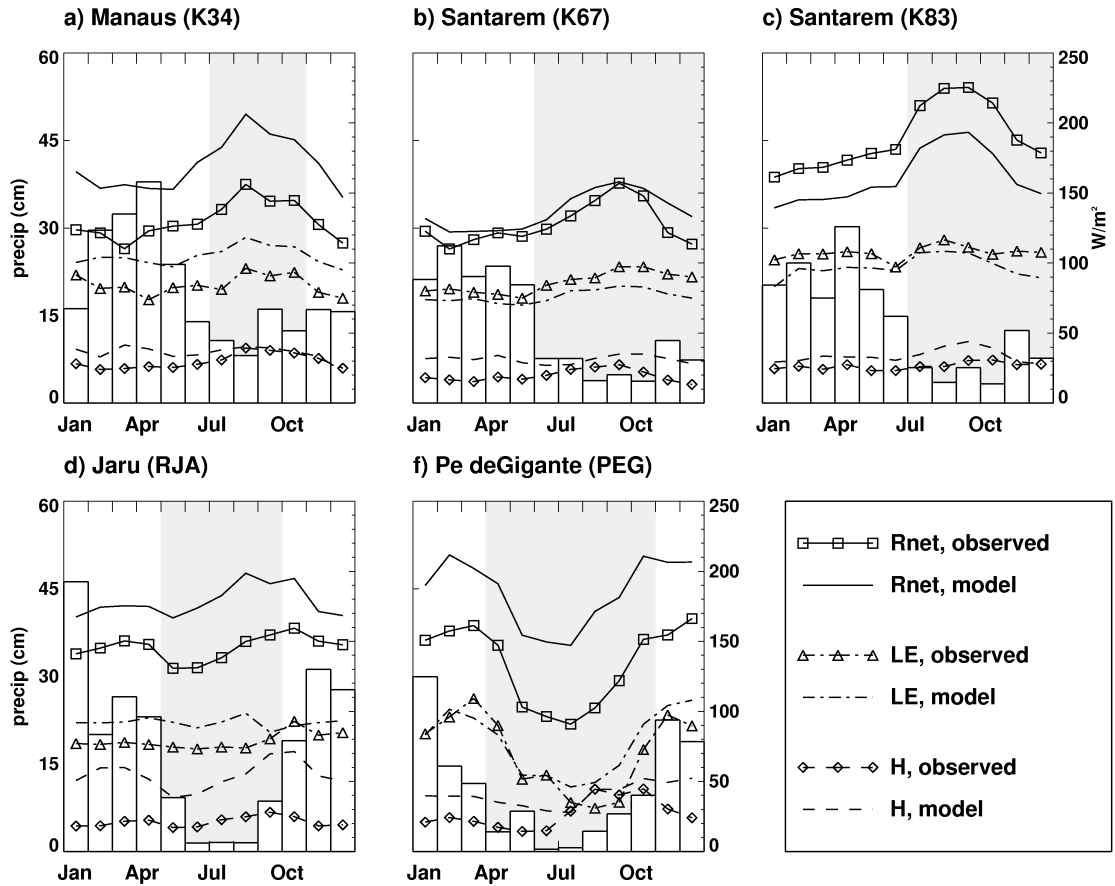|	2000	2001	2002	2003	2004	2005
1: K34			███	███	███	███
2: K67			███	███	███	
3: K83		███	███	███		
4: RJA	███	███	███			
5: PEG		███	███	███		

Figure 2: Data availability for the sites used in this study.

Figure 3: Mean annual cycles of modeled and observed net radiation (Rnet), latent heat (LE), and sensible heat (H) for the 5 stations superimposed on a histogram of monthly-mean precipitation. Locations are shown in Figure 1, dry season is shaded as before.
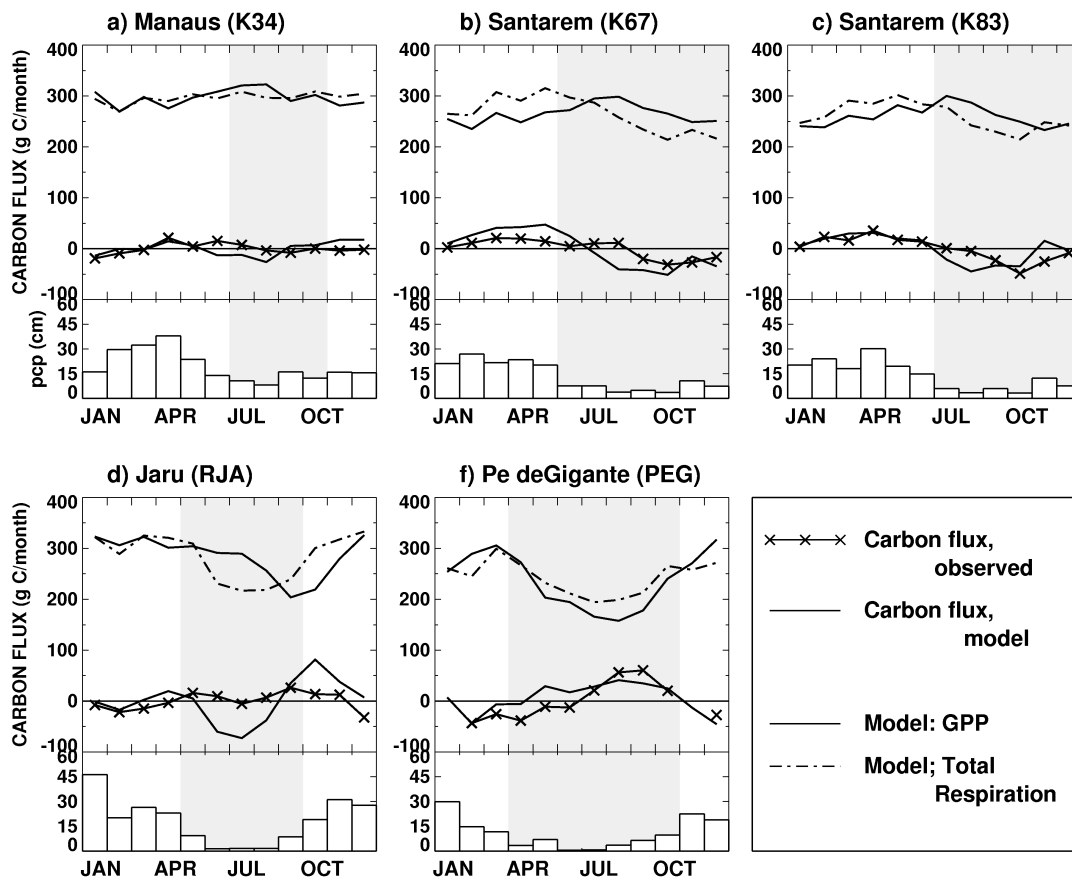
Figure 4: Mean annual cycles of modeled and observed carbon flux for the 5 stations, superimposed on a histogram of monthly-mean precipitation. Locations of towers are shown in Figure 1. Modeled Gross Primary Productivity (GPP) and total respiration are shown at the top of each panel; dry season is shaded.
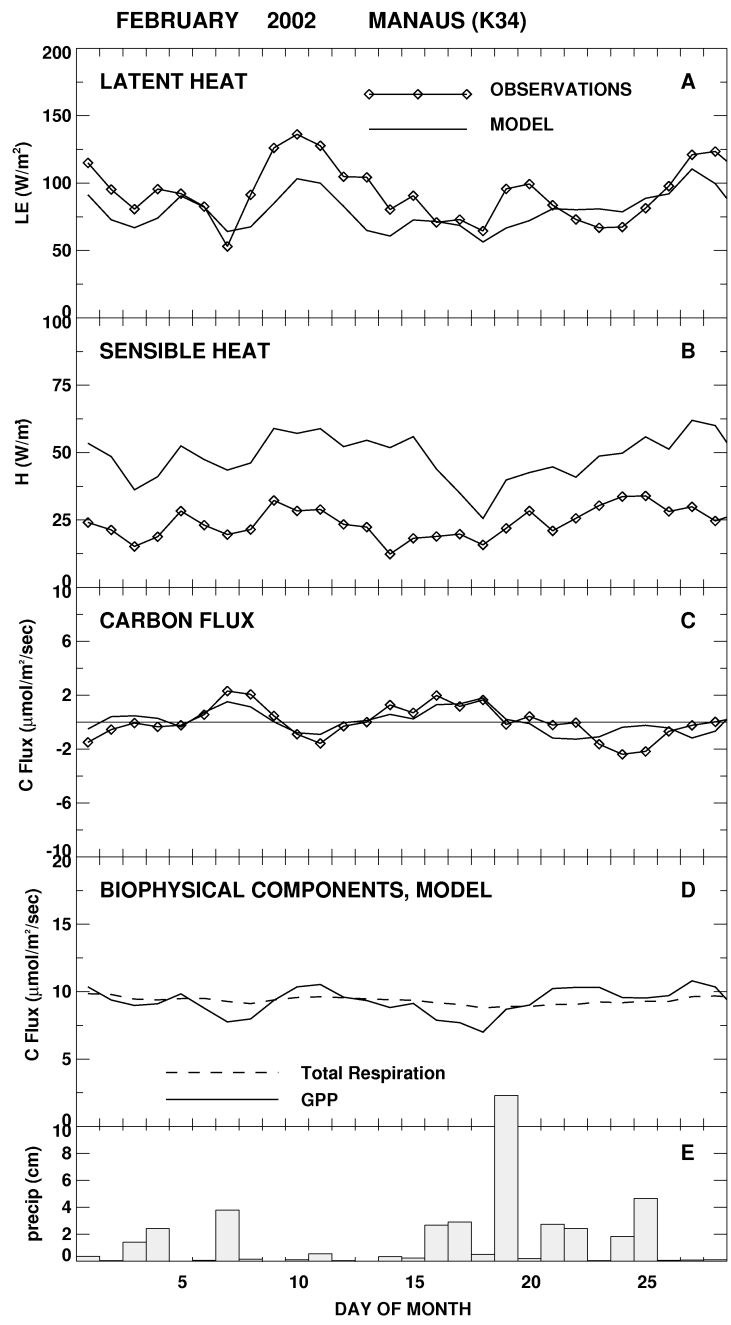
Figure 5: Daily mean (modeled and observed) Latent, Sensible and Carbon flux for the month of February 2002 at K34 (Panels A-C) Observations are shown as solid lines with symbols, simulated value as solid lines. Modeled partition of Carbon flux is shown in Panel D, daily precipitation in Panel E.
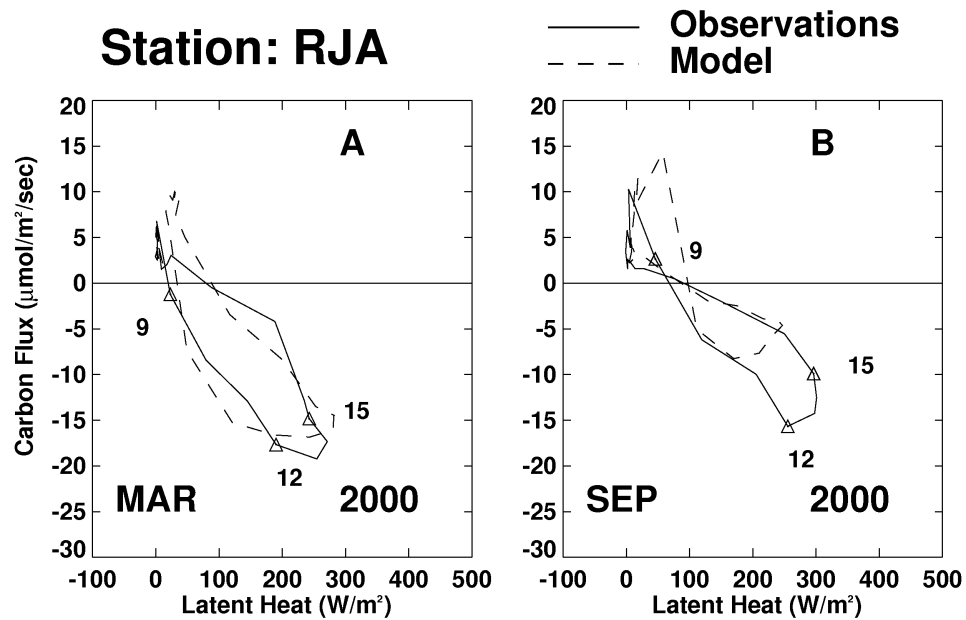
Figure 6: Monthly-mean diurnal composite of Latent Heat (X-axis) plotted against Carbon flux (Y-axis) for RJA, March (panel A) and September (panel B) 2000. Hours 9, 12, and 16 are indicated with triangles in the observations.